published: Mat. Symp. Proc. vol 342 (1994).

GROWTH AND PHOTOLUMINESCENCE OF STRAINED $< 110 >$ $Si/Si_{1-x}Ge_x/Si$ QUANTUM WELLS GROWN BY RAPID THERMAL CHEMICAL VAPOR DEPOSITION

C. W. LIU*, J.C. STURM*, Y. R. J. LACROIX**, M. L. W. THEWALT**, AND D. D. PEROVIC***
*Princeton University, Department of Electrical Engineering, Princeton, NJ 08544
**Simon Fraser University, Department of Physics, British Columbia V5A 1S6, Canada
***University of Toronto, Department of Metallurgy and Material Science, Toronto, Ontario M5S 1A4, Canada

ABSTRACT

We report the first chemical vapor deposition growth and systematic photoluminescence study of strained $Si_{1-x}Ge_x$ alloy layers on $< 110 >$ Si substrates. Compared to $< 100 >$ Si substrates, the same growth conditions yielded a slightly lower Ge composition, but a much lower growth rate. For thick layers, the relaxation along $[1\bar{1}0]$ direction is insufficient and lead to predominantly uniaxial strain in the the films. From the photoluminescence, the bandgap of strained $Si_{1-x}Ge_x$ on $< 110 >$ Si for $0.16 \leq x \leq 0.43$ is determined and compared to theory. A strong "no-phonon" emission process in photoluminescence spectra of strained $< 110 >$ $Si/Si_{1-x}Ge_x/Si$ was observed as compared with that observed in $< 100 >$ layers. Finally, quantum confinement shift of $Si/Si_{0.71}Ge_{0.29}/Si$ wells with a confinement energy up to 110 meV has been observed by varying the well width from 133 Å to 17 Å.

INTRODUCTION

The growth and optical properties of $Si_{1-x}Ge_x$ on Si $< 100 >$ oriented substrates have been widely studied, but little work has been done on other substrate orientations. In this paper, we report the rapid thermal chemical vapor depostion (RTCVD) growth of $Si_{1-x}Ge_x$ alloys on $< 110 >$ silicon substrates and photoluminescence study of such alloys in quantum well structures. The $< 110 >$ strained $Si_{1-x}Ge_x/Si$ heterojunction is of great interest because the orientation of strain can dramatically change the conduction band minima of strained $Si_{1-x}Ge_x$ on Si. For example, on $< 100 >$ Si substrates, four conduction band minima of strained $Si_{1-x}Ge_x$ move down in energy and two move up, on $< 110 >$ substrates the opposite is predicted. Six conduction band minima remain degenerate on $< 111 >$ substrates. Moreover, the $< 110 >$ substrate has the largest predicted conduction band offset (for type I alignment) between strained $Si_{1-x}Ge_x$ and Si among these three substrate orientations [1].

GROWTH

The samples studied by previous work [2−4] were grown by molecular beam epitaxy (MBE). All samples reported in this paper were grown by RTCVD on 100 mm wafers (except sample 1361 on a 75 mm wafer). The Si layers were grown at a nominal temperature of 700 °C from dichlorosilane (DCS), and the $Si_{1-x}Ge_x$ layers were grown at a nominal temperature of 625 °C from germane and DCS. An anomalously low growth temperature on sample 1361 may explain unexpectedly large Ge fraction (43 %) on that sample. The growth pressure was 6 torr, the gas flows were 3 slpm for a hydrogen carrier and 26 sccm for dichlorosilane, and the germane mixture flow (0.8 % in hydrogen) varied from 100 to

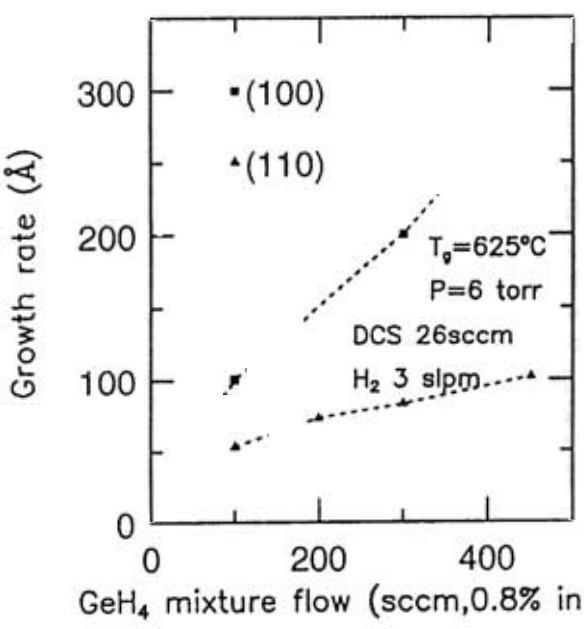

Fig.1. Growth rate of SiGe vs GeH_4 flow on (110) and (100) Si substrates. Compared to (100) Si, the growth rate on (110) Si is lower.

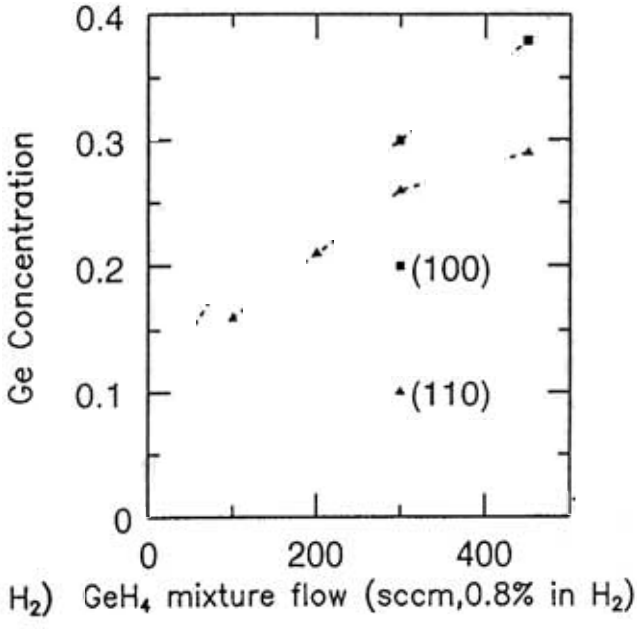

Fig.2. Ge concentration of SiGe vs GeH_4 flow on (110) and (100) Si. The growth condition is the same as in Fig.1.

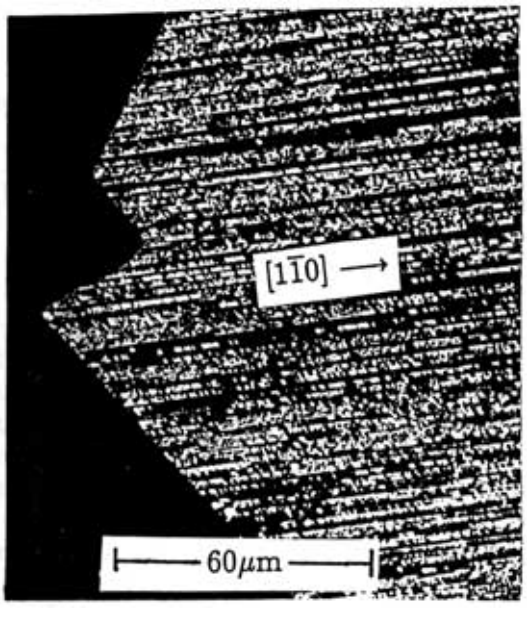

Fig.3. Nomarski micrograph of a 0.5μm $Si_{.71}Ge_{.29}$ relaxed layer. Dislocations only in one direction were observed.

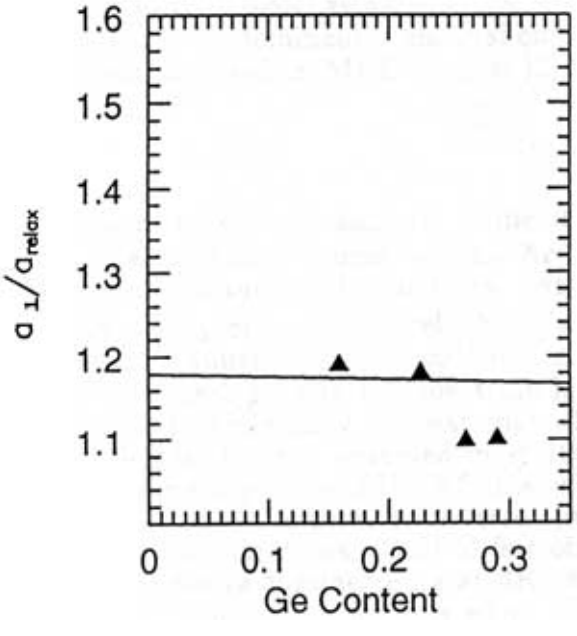

Fig.4. The ratio of measured vertical lattice constant of thick annealed (110) SiGe to that predicted for a relaxed layer for different Ge fraction. The solid line is the theoretical curve for uniaxially strained layers.

450 sccm. The details of the RTCVD reactor can be found in Ref.5. For samples characterized by photoluminescence, the $Si_{1-x}Ge_x$ layers were capped with $\sim$ 100Å of silicon. Previous experiments on < 100 > samples in our lab have shown that a Si cap increases the photoluminescence intensity by over an order of magnitude, presumably due to a decrease in surface recombination [12].

The thickness of $Si_{1-x}Ge_x$ quantum wells sample were measured by cross-sectional transmission electron microscopy (XTEM). The strained $Si_{1-x}Ge_x$ layers were observed by XTEM to be abrupt within 0.3-0.4 nm, similar to < 100 > layers of similar thickness grown either by CVD or MBE techniques [13]. Moreover, all of the quantum wells were defect-free on the scale of XTEM. Using this thickness, and the integrated atomic areal density of Ge from Rutherford Backscattering Spectroscopy (RBS), assuming that atomic density of $Si_{1-x}Ge_x$ is a linear function of Ge content, and assuming abrupt interfaces, we obtained the Ge content in the quantum wells. The measured growth rate and Ge content vs germane mixture flow are plotted in Fig.1 and Fig.2, respectively, with the results on < 100 > substrates. Both the Ge content and the growth rate increase as germane flow increases. Compared to < 100 > Si substrates, the same growth conditions yielded $Si_{1-x}Ge_x$ layers with a slightly lower Ge content, but much lower growth rates (a factor of 2-3 lower).

To study the relaxation of the SiGe films on < 110 > Si, we investigated the morphology and the X-ray diffraction (XRD) on thick layers ($\geq 0.5\mu$m) grown under the same conditions as the quantum well samples and annealed at 900°C to promote relaxation. The plane-view Nomarski micrographs (Fig.3) of the thick (110) $Si_{1-x}Ge_x$ films revealed only one set of dislocation replica along [001] direction (the dislocation line parallel to $[1\bar{1}0]$ dircetion), indicating the relaxation on the orthogonal $[1\bar{1}0]$ direction was retarded. The vertical lattice constant measured from (440) peaks of XRD spectra, normalized with respect to the relaxed (bulk) lattice constant of $Si_{1-x}Ge_x$ for different Ge content (x determined from quantum well samples) is shown in Fig.4. The vertical lattice constants are systematically 10-20 % larger than the relaxed lattice constant. The theoretical ratios of the vertical lattice constant to the relaxed one calculated from elasticity theory are 1.5 and 1.18 for the fully biaxial strained lattice and the fully uniaxial strained lattice (along $[1\bar{1}0]$), respectively. This further confirms the relaxation is predominantly uniaxial on thick $Si_{1-x}Ge_x$ layers grown on Si. Similar results have been observed on MBE samples [2].

PHOTOLUMINESCENCE

The 4K and 77K photoluminescence (PL) were taken with samples immersed in liquid helium and liquid nitrogen, respectively. The excitation source was an Ar^+ ion laser. All the samples in the PL measurement were quantum well structures. At 4K, the PL spectrum of a 23 Å strained < 110 > $Si/Si_{.57}Ge_{.43}/Si$ quantum well (Fig.5(a)) is qualitatively similar to what has been reported in < 100 > substrates [6, 7], and presumably due to shallow bound exciton recombination. The strongest peak in the spectrum is the no-phonon (NP) transition due to the lattice disorder (mainly alloy fluctuations) which relaxes the momentum conservation requirement. Similar to that observed in < 100 > wells, there are four phonon-assisted replicas at the lower energy side of the NP line, which are attributed to the transverse acoustical (TA) phonon and the three transverse optical (TO) phonon replicas related to Si-Si, Si-Ge, and Ge-Ge vibrations. Only a few of the quantum wells exhibited such strong well-resolved band-edge luminescence at 4K, while all of them exhibited band-edge luminescence at 77K. The reason for this effect is not clear, but may be related to nonradiative traps due to an intermittent vacuum integrity or gas purity problem in the CVD reactor. In any case, this effect was also observed in samples grown on < 100 > substrates at the same time frame as these samples, so it is not unique to the < 110 > orientation. As a result, the bandgaps were extracted from the 77K PL spectra. The 77K PL spectrum (pump power density $\sim$ 20 W/cm^2) for the same sample of Fig.5(a) is shown in Fig.5(b). At 77K, thermal broadening and a band-filling effect due to the pump power lead to broad overlapping peaks (Fig 5(b)). To extract

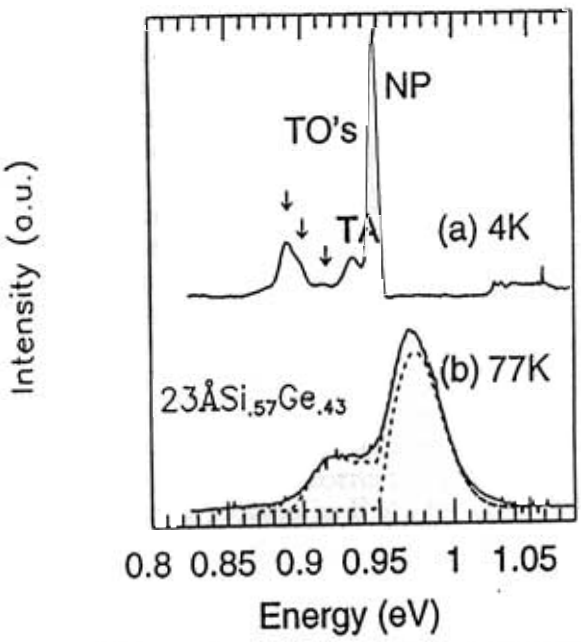

Fig.5. PL spectra at 4K and 77K. The dotted lines are the theoretical fitting of electron hole plasma model and the no-phonon component of the model (the onset at low energy side is the bandgap).

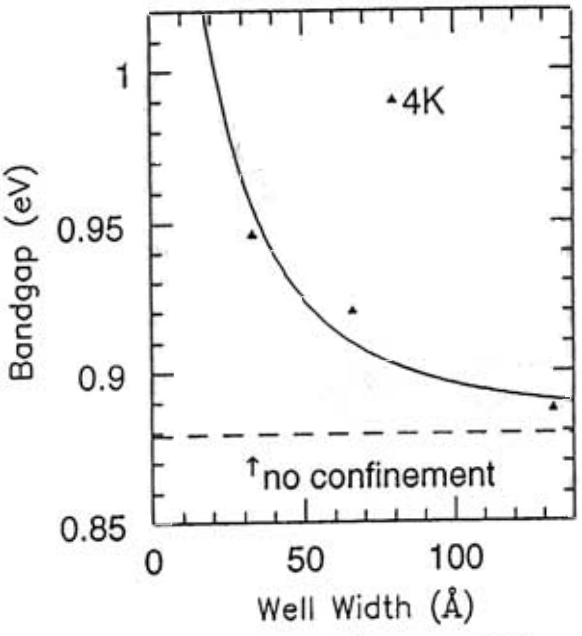

Fig.6. The quantum confinement shift measured by 4K PL. The solid line is the fitting using the assumptions described in text. The dotted line indicates the bandgap after quantum confinement correction.

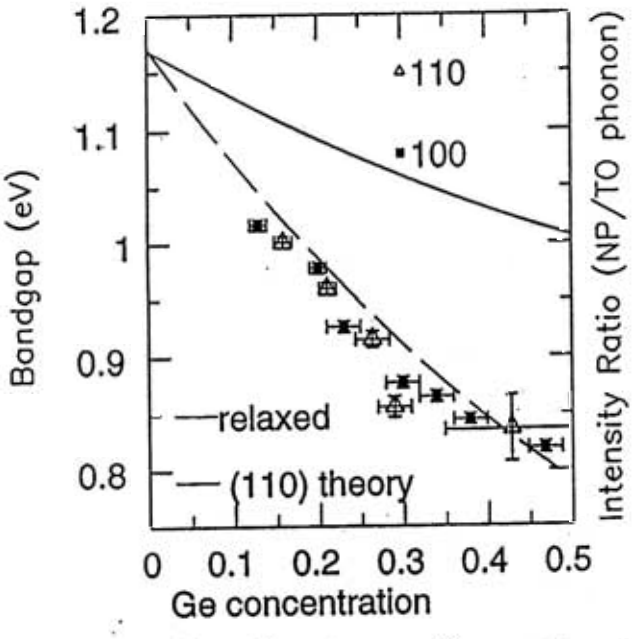

Fig.7. The plot of bandgap vs Ge concentration for both strained (110) and (100) $Si_{1-x}Ge_x$ alloys measured from 77K PL. The dotted line is the prediction of People et at. The solid line is the relaxed bandgap.

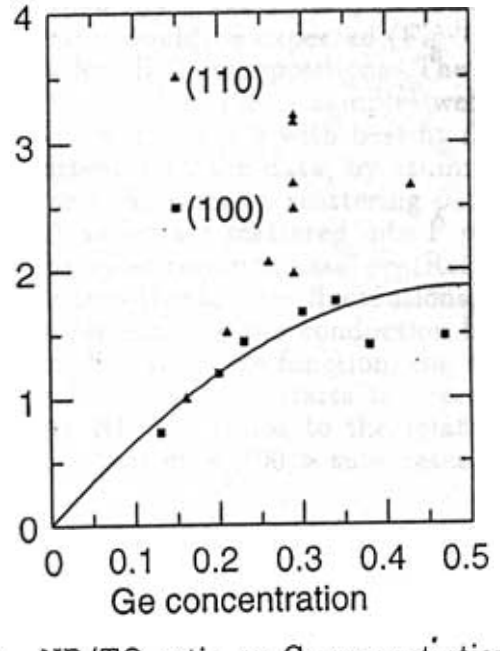

Fig.8. NP/TO ratio vs Ge concentration of strained (110) and (100) quantum wells. The (110) wells have higher ratios, compared to (100) wells.

a bandgap, the 77K PL spectra were fitted using an electron-hole plasma model (EHP). The details of this model is given in Ref.8. The fitted spectra are shown in Fig.5(b) as well as the contribution from the NP line only. The bandgap is the lower edge of this component. Note that the bandgap obtained from 77K PL (Fig.5.(b)) is very close to the energy position of NP line (excitonic bandgap) in 4K PL (Fig.5(a)) of the same sample. To determine the "true bandgap" of strained < 110 > $Si_{1-x}Ge_x$, we have to calculate the quantum confinement energies of both holes and electrons. We assumed a square potential profile, a theoretical valence band discontinuity $\Delta E_v = 0.71x$ [1], the measured quantum well thickness, the hole effective mass of 0.28 m_o [10], and the electron effective mass of 0.19 m_o. The quantum confinement effect has been observed with $Si/Si_{0.71}Ge_{i0.29}/Si$ quantum wells with different well width. Fig.6 plots the excitonic bandgap gap from 4K PL vs well width with the theoretical curve using these parameters. A quantum confinement energy up to of 110 meV was observed by varying the well width from 133Å to 17Å. Fig.7 displays a plot of the bandgap of strained < 110 > $Si_{1-x}Ge_x$ versus Ge content after corrections for quantum confinement as well as the bandgap of strained < 100 > $Si_{1-x}Ge_x$ layers after quantum confinement correction. The data is very close to the theoretical curve of People et al., which is plotted in Fig.7 for comparison along with the bandgap of relaxed $Si_{1-x}Ge_x$ [9]. Although the bandgap of strained $Si_{1-x}Ge_x$ on < 110 > substrates is predicted to be slightly lower than that on < 100 > substrates (approximately 15 meV lower for x=0.4 [1]) , within experimental resolution of E_g and x, we can not observe such a shift in a comparison of the 77K PL of < 100 > and < 110 > samples grown in our lab. The details of the sample structures and best-fit parameters for each samples are given in Ref.15.

It is interesting to note that in these < 110 > strained layers, the integrated NP/TO ratio was substantially stronger than that observed in comparable < 100 > structures. Fig.8 plots the fitted ratio of the NP line strength to the total strength of TO lines vs Ge fraction for both < 110 > and < 100 > samples at 77K, where impurity localization is not expected to affect the NP/TO ratio. Note that the different data points for the same Ge concentration are due to different well widths. All the < 100 > samples have the thickness more than 100 Å, for which a high NP/TO ratio would be expected (Fig.9). It is obvious that < 110 > has higher ratios than < 100 > for all Ge compositions. The well width dependence of the NP/TO ratios for both < 110 > and < 100 > samples wells is shown in Fig.9. The relative alloy scattering rate vs well width (Fig.9 with best-fit ΔE_c) calculated from eqn.109 in Ref.14 is qualitatively consistent with the data, by asumming phonon scattering rates are constant for all the wells and the electron scattering path is dominant for the NP transition, i.e. electrons in the Δ valley are scattered into Γ point in k space and then, recombine with holes (which is the most common case, see Ref.16). Because a more concentrated wave function will be more sensitive to alloy fluctuations, the alloy scattering rate increases as either the well width decreases or the conduction band offset increases. However, if the width is too small to confine the wave function, the wave function will spread into the Si barriers and thus, the scattering rate starts to decrease. Therefore, we tentatively attribute the relatively larger NP/TO ratios to the relatively larger conduction band offset on < 110 > substrates than that on < 100 > substrates.

SUMMARY AND ACKNOWLEDGEMENT

We have reported the growth of strained < $1\bar{1}0$ > $Si_{1-x}Ge_x$ by CVD, and used the photoluminescence spectroscopy to measure the bandgap of strained < 110 > $Si_{1-x}Ge_x$ on Si. Our results are in good agreement with the prediction of People et al.[11], but the small predicted difference between the bandgap of films strained on < 110 > vs < 100 > substrates has not been resolved within experimental error. The no-phonon luminescence of the < 110 > films is relatively stronger than that on < 100 > substrates, evidence of the relatively larger conduction band offset of strained $Si_{1-x}Ge_x$ on < 110 > substrates, compared to < 100 > substrates.

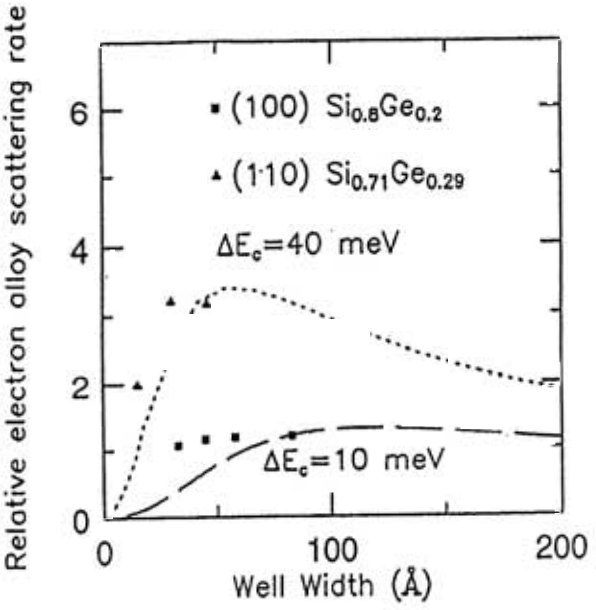

Fig.9. The NP/TO ratio vs well width for both (110) and (100) samples. The fitting of (110) data required a higer value of ΔE_c than that of (100) data.

The RBS assistance of H. Gossmann (AT&T Bell Labs) and A. St Amour (Princeton University), and the support of ONR (N00014-90-J-1316) and NSF are gratefully appreciated. The work of Simon Fraser University was supported by the National Science and Engineering Research Council of Canada.

REFERENCE

1. C.G. Van de Walle and R.M. Martin, *Phys. Rev.* B34, 5621 (1986).
2. R. Hull, J. C. Bean, L. Peticolas, and D. Bahnck, *Appl. Phys. Lett.* 59, 964 (1991).
3. Chanho Lee and K. L. Wang *Appl. Phys. Lett.* 60, 2264 (1992).
4. Susumu Fukatsu, Noritaka Usami and Yasuhiro Shiraki, *Jpn. J. Appl. Phys.* 32, 1502 (1993).
5. J.C. Sturm, P.V. Schwartz, E.J. Prinz, and H. Manoharan, J. Vac. Sci. Tech., B9, 2011 (1991).
6. J.C. Sturm, H. Manoharan, L.C. Lenchyshyn, M.L.W. Thewalt, N.L. Rowell, J.-P. Noël, and D.C. Houghton, *Phys. Rev. Lett.* 66, 1362 (1991).
7. D.J. Robbins, L.T. Canhan, S.J. Barnett, A.D. Pitt, and P. Calcott, *J. Appl. Phys.* 71, 1407 (1992).
8. X. Xiao, C.W. Liu, J. C. Sturm, L. C. Lenchyshyn, and M.L.W. Thewalt, *Appl. Phys. Lett.* 60, 1720 (1992).
9. J. Weber and M.I. Alonso, *Phys. Rev.* B40, 5683 (1989).
10. X. Xiao, C.W. Liu, J. C. Sturm, L. C. Lenchyshyn, M.L.W. Thewalt, R.B. Gregory, and P. Fejes, *Appl. Phys. Lett.* 60, 2135 (1992).
11. R. People, J. C. Bean, and D. V. Lang, in *Semiconductors and Semimetals, Vol.32, Strained-Layer Superlattice: Physics*, edited by T. P. Pearsall, p141 (Academic Press, New York, 1990).
12. J.C. Sturm, X. Xiao, P. V. Schwartz, and C. W. Liu, J. Vac. Sci. Tech., B10, 1998 (1992).
13. D.D. Perovic, G.C. Weatherly, and D.C. Houghton, Philos. Mag., 64, 1 (1991).
14. G. Bastard, in Wave mechanics applied to semiconductor heterostructures, (Halsted Press, New York, 1988), p. 221.
15. C.W. Liu, J.C. Sturm, Y. R. J. Lacroix, M. L. W. Thewalt, and D. D. Perovic, to be published *Appl. Phys. Lett.* (1994).
16. B.K. Ridley, in Quantum process in semiconductors, 2nd ed. (Clarendon press, Oxford, 1988) p.214.